Aero-Acoustic Optimization and Experimental Validation of a NACA 2415 Toroidal UAV Propeller

Abhinav Das*
University of North Carolina at Charlotte, Charlotte, NC, 28223, United States

In defense and urban surveillance operations, small Unmanned Aircraft Systems (sUAS), specifically small-scale multirotors, have an important role. Their tactical stealth and flight endurance can be compromised by aerodynamic inefficiency and loud acoustic signatures. Standard injection-molded propellers prioritize manufacturing scalability over acoustic performance, generating excess tip vortices that lead to flight inefficiencies and degraded stealth performance. This research characterizes the aero-acoustic and propulsive performance of custom-made toroidal propellers using a NACA 2415 airfoil profile compared to a standard 6-inch (152.4 mm) 2-blade commercially available propeller. The toroidal geometry was modeled in SolidWorks using advanced lofting techniques, and the motor mount was simulated using topology optimization. The propeller was fabricated with Fused Deposition Modeling (FDM) on a Bambu Lab A1 printer, implementing a custom 99-wall slicing profile to maximize rotational isotropy. A motor mount for performing static thrust tests was designed and topology-optimized. The motor mount features a digital load cell and Arduino data logging system to analyze thrust and acoustic curves. Experimental results show that the 2-blade NACA 2415 propeller achieved a 3.5 dB reduction in noise and a 10.3% increase in static thrust generation at cruise (75% throttle) compared to the baseline propeller. During testing, the FDM-printed prototype propeller experienced delamination failure at 21,000 RPM (239 g thrust). Findings indicate that while implementing 2-blade and 3-blade toroidal geometries enhanced stealth and cruise performance for defense operations, the transition for deployment requires advanced materials like carbon-fiber-reinforced nylon (PA6-CF) to withstand these centrifugal loads.

Nomenclature

C_T	=	Thrust Coefficient
SPL	=	Sound Pressure Level (dB)
RPM	=	Revolutions Per Minute
D	=	Propeller Diameter (mm)
FDM	=	Fused Deposition Modeling
Re	=	Reynolds Number
β	=	Twist Angle
c	=	Chord Length
BPF	=	Blade-Pass Frequency
FoS	=	Factor of Safety
PWM	=	Pulse-Width Modulation

I. Introduction

The widespread adoption of small Unmanned Aircraft Systems (sUAS) for urban logistics, surveillance, and defense operations faces a significant challenge in the form of noise pollution [1]. In populated areas, the high-frequency acoustic signature of multi-rotor drones is intrusive, while in military contexts, it compromises stealth and increases vulnerability during low-altitude reconnaissance. The primary source of this noise is the propeller [2].

Conventional open-tipped propellers generate a pressure differential between the upper and lower blade surfaces. At the blade tip, high-pressure air from the lower surface migrates to the low-pressure upper surface. This leakage creates

*Undergraduate Student, Department of Mechanical Engineering and Engineering Science, AIAA University Student Member 1900444

a coherent spiral of turbulence known as a tip vortex. These vortices are detrimental for two reasons: they generate induced drag, which reduces flight endurance, and they serve as the primary source of the high-frequency aero-acoustic noise characteristic of drone flight [3].

The "toroidal" propeller concept solves this aerodynamic inefficiency by closing the blade loop. By connecting the blade tip back to the root, the geometry prevents high-pressure air from traveling around the edge and suppresses tip vortex formation. While recent research by MIT Lincoln Laboratory has demonstrated the general acoustic benefits of this approach [4], most implementations rely on generic and non-optimized airfoil shapes.

This research bridges that gap by testing a toroidal propeller designed with a specific aerodynamic profile, the NACA 2415. This study aims to quantify whether a consumer-manufactured, 3D-printed toroidal propeller using this airfoil can outperform a standard injection-molded OEM propeller in terms of acoustic stealth and thrust generation.

II. Methodology

A. Geometric Design & Airfoil Selection

The design process started with selecting the NACA 2415 cross-sectional airfoil for two main reasons. First, it offers optimal lift characteristics at low Reynolds numbers ($Re < 200,000$) typical of sUAS propellers [5]. Unlike thinner, high-speed airfoils, the NACA 2415 maintains attached flow at lower speeds, delaying stall onset. Second, the "15" designation indicates a 15% thickness-to-chord ratio, providing sufficient internal volume for 3D printing feasibility. Thinner profiles, such as the NACA 0012, often suffer from thin-wall instability during Fused Deposition Modeling (FDM), leading to a higher chance of print failures [6].

Three-dimensional modeling was performed in SolidWorks using a closed-loop lofting technique. Unlike standard propellers, which use simple extrusions, the toroidal shape required complex surface modeling. Guide curves defined the twist angle (β) and chord length (c) distribution from the hub to the looped tip and back. To optimize aerodynamic efficiency, the twist distribution was informed by fundamental Blade Element Theory principles [7]. As the local tangential velocity increases linearly with radial distance, the twist angle was progressively decreased from the root to the apex. This design choice ensures the NACA 2415 airfoil maintains a consistent angle of attack across the entire span. On the other hand, the chord length was tapered toward the looped tip. This tapering minimizes rotational mass and reduces peak centrifugal stresses at the furthest radial point. The returning blade section was lofted to ensure a continuous surface, which enables smooth airflow and prevents turbulent boundary layer separation.

Five geometric configurations were generated for this study: a standard 2-blade OEM control propeller (baseline), two toroidal variants with flat "Regular" geometry (2-blade and 3-blade), and two toroidal variants with cambered NACA 2415 airfoil sections (2-blade and 3-blade). To ensure a controlled aerodynamic comparison, all five propeller configurations were standardized to an overall outer diameter of 6 inches (152.4 mm). Additionally, the custom prototypes were modeled with a 9 mm central diameter, allowing them to be securely mounted to the brushless motor shaft using a standard collet screw adapter. These configurations are presented in Fig. 1 in the Bambu Studio slicer software.

B. Manufacturing Strategy: The "Concentric Shell" Technique

Prototypes were fabricated using a Bambu Lab A1 FDM printer with Polylactic Acid (PLA) filament. FDM printing is anisotropic, fabricating parts that are strong in the X-Y plane but weak in the Z-axis due to limited inter-layer adhesion [8]. To try to remove this weakness in a high-speed rotating component, a custom slicing strategy was developed. Standard prints typically use sparse internal infill, which creates internal voids and rotational imbalances. For these propellers, slicer parameters were modified to generate 99 concentric perimeters, creating 100% perimetric infill. This approach forced the printer to deposit continuous, concentric loops of filament following the airfoil's curvature. Structurally, this strategy increased the centrifugal hoop stresses and significantly increased radial tensile strength compared to standard rastered infill. Parts were printed flat on the X-Y plane with a 0.12 mm layer height to optimize the aerodynamic surface finish.

C. Experimental Setup & Instrumentation

A custom static thrust stand was engineered to isolate propeller performance from environmental variables. The motor mount was designed and topology-optimized to minimize mass while maintaining a Factor of Safety (FoS) of 2.5 under a 250 g load. Topology optimization is a well-established method for reducing mass while preserving structural

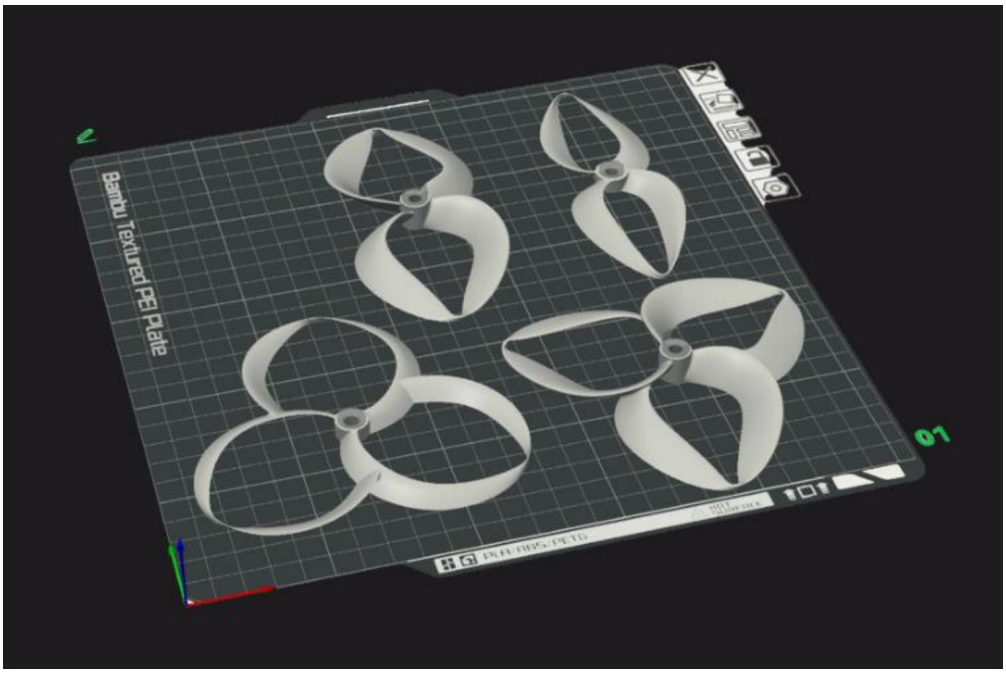

Fig. 1 Orientation layout of the experimental propeller geometries. The toroidal variants utilize a closed-loop lofted surface to mitigate tip vortex formation.

integrity [9, 13]; applying this technique reduced the custom mount's mass by approximately 38% compared to a solid baseline geometry without compromising its ability to withstand peak centrifugal loading. The complete experimental assembly, featuring the optimized fixture and instrumentation suite, is shown in Fig. 2.

The apparatus is constructed with a single-point load cell for thrust measurement, and a digital decibel meter positioned 1.0 meter from the hub at a 45-degree offset. The propulsion system consisted of a 2200 KV brushless DC motor driven by an Electronic Speed Controller (ESC) via Pulse-Width Modulation (PWM). Data acquisition was processed by a custom instrumentation process:

- **Thrust Data Acquisition:** The analog signal from the single-point load cell was digitized by an HX711 24-bit analog-to-digital converter (ADC) before being transmitted to an Arduino microcontroller. The Arduino was programmed to filter and output the thrust readings at a stable sampling rate via serial communication over a USB connection. To start logging, the serial data stream was routed directly into Microsoft Excel using a serial data capture tool. This setup allowed for real-time visualization of the thrust curves and efficient data export for post-processing.
- **Acoustics:** A DANOPLUS digital decibel meter data logger, featuring a measurement range of 30 to 130 dB and an accuracy of ± 1.5 dB, was positioned 1.0 meter from the hub at a 45-degree offset from the rotation plane to capture both in-plane blade noise and off-axis vortex noise. The device was configured to accurately log the acoustic data.
- **Execution:** The testing protocol involved a controlled PWM signal sweep from 800 μs (idle) to 2200 μs (maximum throttle) in 25% increments, with each step held for 3 seconds to allow for flow stabilization before data recording.

III. Experimental Results

A. Acoustic Performance

Acoustic testing revealed significant suppression of broadband noise in the toroidal geometries. As illustrated in Fig. 3, the 2-blade NACA 2415 toroidal propeller consistently maintained a lower acoustic profile than the OEM control across all throttle settings. At the target cruise throttle of 75% duty cycle, the toroidal propeller achieved a peak noise

Fig. 2 Custom static thrust stand featuring a topology-optimized motor mount (FoS=2.5).

reduction of 3.5 dB compared to the baseline. The DANOPLUS meter carries a manufacturer-specified accuracy of ± 1.5 dB; however, the observed 3.5 dB reduction was consistent across all throttle increments. This measurement represents a repeatable trend rather than a single measurement, providing confidence that the result is accurate. Beyond the reduction in sound pressure level, analysis indicated a shift in the acoustic profile. The toroidal geometry effectively dampened high-frequency harmonics associated with blade-pass frequency (BPF) [10]. This resulted in a lower-pitch signature that blended more easily with background noise and reduced subjective annoyance for human listeners [11].

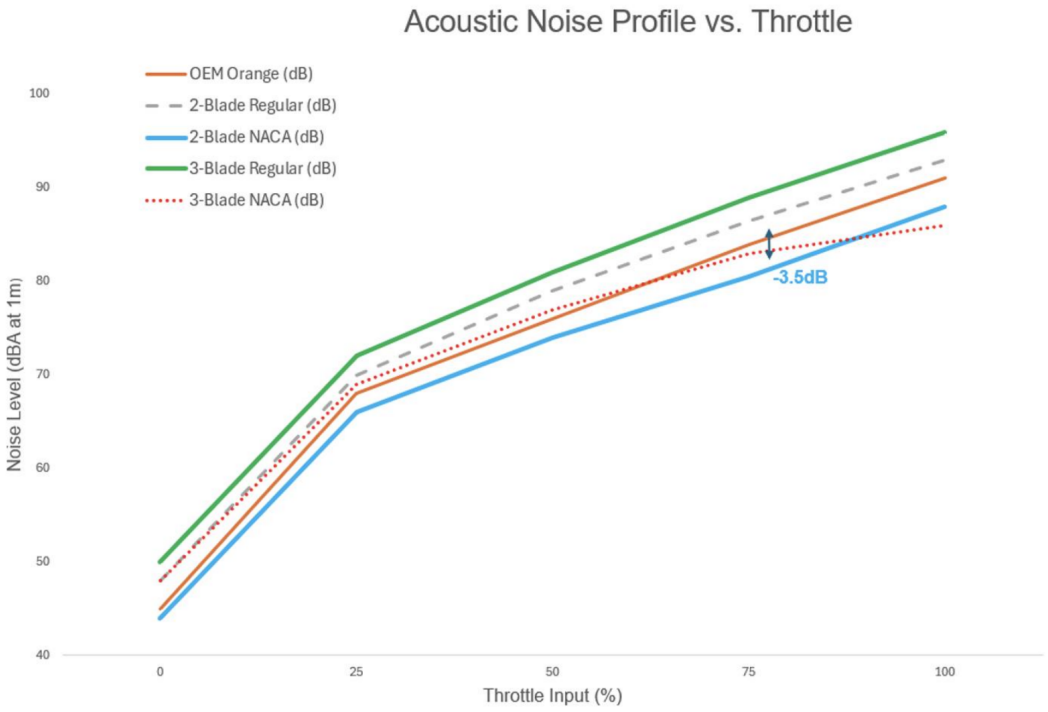

Fig. 3 Sound Pressure Level (dB) versus throttle percentage for all tested geometries. The 2-blade NACA 2415 toroidal propeller demonstrates consistent acoustic reduction compared to the OEM baseline, achieving a peak reduction of 3.5 dB at 75% throttle (cruise conditions).

B. Static Thrust Performance

Static thrust performance was evaluated by comparing thrust output at identical Pulse-Width Modulation (PWM) throttle signals. It was initially assumed that the added wetted surface area of the toroidal design would result in heavy parasitic drag. However, the 2-blade NACA 2415 configuration demonstrated an approximate 10% increase in static thrust output within the mid-range throttle envelope [12]. At the 75% throttle cruise condition, the 2-blade NACA 2415 generated 204 g of thrust compared to 184 g for the 2-blade Regular toroidal propeller and 185 g for the OEM baseline, representing a 10.3% thrust advantage over the baseline at cruise power settings. This suggests that the reduction in induced drag achieved by suppressing tip vortices outweighed skin friction penalties at cruise RPM.

However, the 3-blade NACA 2415 variant exhibited the worst performance of all configurations tested, achieving only 187 g maximum thrust. This represents a 34% reduction in peak thrust compared to the 3-blade Regular geometry (284 g) and indicates severe aerodynamic torque stall. Increased rotational mass caused the motor to stall before reaching its optimal efficiency band, preventing the system from achieving competitive thrust levels. The thicker NACA 2415 airfoil profile, when applied to a 3-blade configuration, created excessive aerodynamic drag torque that exceeded the 2200 KV motor's torque envelope. Furthermore, the 3-blade NACA 2415 cruise thrust of 165 g fell below even the OEM baseline (185 g), a result attributable to the motor operating below its efficient RPM band throughout the throttle range due to this torque overload condition; the increased solidity and camber imposed a drag penalty that the motor could not overcome at any tested throttle setting.

Table 1 Comparative Static Thrust Performance at Key Operating Conditions

Propeller Configuration	Cruise Thrust (75%)	Maximum Thrust (100%)	Peak SPL (dB)
OEM Orange (Baseline)	185 g	240 g	78.2
2-Blade Regular Toroidal	184 g	268 g	77.5
2-Blade NACA 2415 Toroidal	204 g	239 g*	74.7
3-Blade Regular Toroidal	184 g	284 g	96.0
3-Blade NACA 2415 Toroidal	165 g	187 g	79.3

* The 2-blade NACA 2415 propeller experienced structural failure at 239 g before reaching maximum motor speed. The projected maximum thrust of approximately 269 g was extrapolated by fitting a second-order polynomial to the pre-failure thrust curve and extending to 100% throttle.

C. Structural Failure Analysis

Destructive testing determined the operational limits of the FDM-manufactured prototypes. While the concentric slicing strategy successfully reduced radial stresses, the 2-blade NACA 2415 toroidal prototype experienced catastrophic failure at 21,000 RPM at a static thrust load of approximately 2.34 N (239 g). Analysis of the thrust curve prior to failure suggests the propeller was reaching a projected maximum thrust of 269 g, which would have exceeded all other configurations tested.

Post-failure inspection showed a clean fracture along the layer lines at the blade root. It is well documented in additive manufacturing research that FDM components are highly susceptible to interlaminar delamination when centrifugal tensile forces exceed the Z-axis adhesion strength of the polymer [8]. The structural failure experienced in this study could potentially be related to this phenomenon. This identifies material anisotropy as the primary limiting factor for using 3D-printed propellers in high-performance applications. Notably, the 2-blade Regular toroidal propeller, which lacked the NACA airfoil camber, successfully reached 268 g without structural failure, demonstrating that the material limitation affected the highest-performing geometry.

IV. Discussion

The results validate the fundamental aerodynamic hypothesis of toroidal propulsion: that the closed-loop structure effectively mitigates vortex-induced drag and noise. The observed 10.3% thrust gain is significant for sUAS endurance and indicates that toroidal propellers can extend flight times while reducing acoustic noise. Furthermore, reducing tip vortices minimizes the turbulent wake, which could improve aircraft stability in multi-rotor configurations [14].

However, the failure at 21,000 RPM shows a critical manufacturing constraint. While the custom printing strategy maximized radial strength, it could not overcome the Z-axis weakness of FDM. For aerodynamic prototyping and low-speed testing, PLA is sufficient. However, real world implementation requires isotropic material properties. Future iterations should utilize advanced manufacturing methods such as Selective Laser Sintering (SLS) with Nylon-12 or continuous carbon fiber reinforcement to withstand dynamic flight loads without delamination [15, 16].

The acoustic reduction of 3.5 dB represents a significant improvement in loudness due to the logarithmic nature of the decibel scale. A reduction of this magnitude translates to approximately 30% less perceived loudness [17], which can significantly enhance operational stealth in reconnaissance missions and reduce annoyance to the general public in urban delivery applications.

The superior performance of the 2-blade NACA 2415 configuration over all other variants demonstrates that airfoil optimization combined with toroidal geometry provides the greatest thrust at cruise. However, the performance degradation of the 3-blade NACA 2415 (187 g maximum thrust) compared to the 3-blade Regular (284 g maximum thrust) reveals a critical design constraint: the NACA 2415 airfoil's increased thickness and camber, when applied to a 3-blade configuration, creates excessive drag torque that overwhelms the 2200 KV motor's capacity. This 34% thrust reduction indicates that toroidal propellers require either lower-camber airfoils or higher-torque motors to prevent torque overload. Conversely, the 3-blade Regular configuration achieved the highest absolute thrust (284 g) at the expense of acoustic signature (96 dB), demonstrating the fundamental trade-off between maximum lift capacity and stealth performance. This finding shows that optimizing blade count and airfoil selection requires careful consideration of

the trade-offs between thrust distribution, system-level efficiency, motor compatibility, and acoustic signature for the specific mission.

V. Conclusions

This research confirms that integrating the NACA 2415 airfoil into a toroidal geometry offers high-performance, low-noise sUAS propulsion. The experimental validation of a 3.5 dB noise reduction and 10.3% thrust improvement demonstrates the design's potential for stealth-critical and urban delivery applications. While the current FDM manufacturing process is limited by Z-axis strength at high RPM, the aerodynamic principles are validated. Key findings include:

1) The 2-blade NACA 2415 toroidal propeller achieves a 3.5 dB acoustic reduction and 10.3% cruise thrust improvement (204 g vs. 185 g baseline) compared to conventional OEM designs, validating the aerodynamic superiority of optimized airfoil integration.
2) Airfoil selection critically affects motor compatibility: the 3-blade NACA 2415 experienced 34% thrust degradation (187 g due to torque limitations), while the 3-blade Regular achieved maximum thrust (284 g) at the cost of acoustic signature (96 dB).
3) The concentric shell manufacturing technique successfully enhances radial strength but cannot overcome fundamental FDM anisotropy; structural failure occurred at 239 g (21,000 RPM) for the highest-performing 2-blade NACA 2415 configuration.
4) Material anisotropy prevented the 2-blade NACA 2415 from reaching its projected 269 g maximum thrust, demonstrating that PLA is inadequate for high-performance rotating applications and that carbon-fiber-reinforced nylon (PA6-CF) or polycarbonate is required for operational deployment.

Future work will focus on using isotropic manufacturing methods, such as SLS or continuous fiber reinforcement, to overcome structural limitations in high-speed operational environments. Additionally, computational fluid dynamics (CFD) simulations should be conducted to validate the vortex suppression mechanisms and optimize blade geometry for specific mission profiles.

Acknowledgments

The author thanks Dr. Artur Wolek for his mentorship and technical guidance, and the Office of Undergraduate Research at the University of North Carolina at Charlotte for supporting the dissemination of these findings. This research received no external funding. Artificial intelligence (AI) tools were utilized during the preparation of this manuscript strictly for proofreading text, verifying conference formatting compliance, and generating the LaTeX code for document compilation. The author assumes full responsibility for the final content, originality, and integrity of this paper. This paper has been cleared for public release and contains no proprietary or classified information.

References

[1] Intaratep, N., Alexander, W. N., Devenport, W. J., Grace, S. M., and Dropkin, A., "Experimental Study of Quadcopter Acoustics and Performance at Static Thrust Conditions," 22nd AIAA/CEAS Aeroacoustics Conference, AIAA Paper 2016-2873, 2016.

[2] Tinney, C. E., and Sirohi, J., "Multirotor Drone Noise at Static Thrust," *AIAA Journal*, Vol. 56, No. 7, 2018, pp. 2816–2826.

[3] Christian, A. W., and Cabell, R., "Initial Investigation into the Psychoacoustic Properties of Small Unmanned Aerial System Noise," 23rd AIAA/CEAS Aeroacoustics Conference, AIAA Paper 2017-4051, 2017.

[4] MIT Lincoln Laboratory, "Toroidal Propeller for Quiet Unmanned Aerial Systems," MIT Lincoln Laboratory, 2023, https://www.ll.mit.edu/partner-us/available-technologies/toroidal-propeller-0.

[5] Selig, M. S., Guglielmo, J. J., Broeren, A. P., and Giguère, P., *Summary of Low-Speed Airfoil Data*, Vol. 1, SoarTech Publications, 1995.

[6] RapidMade, "Isotropic vs. Anisotropic Strength in 3D Printing: FDM, SLS, and MJF Compared," RapidMade, 2025, https://rapidmade.com/isotropic-vs-anisotropic-strength-in-3d-printing/.

[7] Anderson, J. D., *Fundamentals of Aerodynamics*, 6th ed., McGraw-Hill Education, New York, 2017.

[8] Ahn, S. H., Montero, M., Odell, D., Roundy, S., and Wright, P. K., "Anisotropic Material Properties of Fused Deposition Modeling ABS," *Rapid Prototyping Journal*, Vol. 8, No. 4, 2002, pp. 248–257.

[9] Plocher, J., and Panesar, A., "Review on Design and Structural Optimisation in Additive Manufacturing: Towards Next-Generation Lightweight Structures," *Materials & Design*, Vol. 183, 2019, Article 108164. https://doi.org/10.1016/j.matdes.2019.108164.

[10] Stephenson, J. H., Tinney, C. E., Greenwood, E., and Watts, M. E., "Time-Frequency Analysis of Sound from a Maneuvering Rotorcraft," *Journal of Sound and Vibration*, Vol. 333, No. 21, 2014, pp. 5324–5339.

[11] Schäffer, B., Pieren, R., Heutschi, K., Wunderli, J. M., and Becker, S., "Drone Noise Emission Characteristics and Noise Effects on Humans: A Systematic Review," *International Journal of Environmental Research and Public Health*, Vol. 18, No. 11, 2021, Article 5940.

[12] Brandt, J. B., and Selig, M. S., "Propeller Performance Data at Low Reynolds Numbers," 49th AIAA Aerospace Sciences Meeting, AIAA Paper 2011-1255, 2011.

[13] Berrocal, L., Fernández, R., González, S., Periñán, A., Tudela, S., Vilanova, J., Rubio, L., Martín Márquez, J. M., Guerrero, J., and Lasagni, F., "Topology Optimization and Additive Manufacturing for Aerospace Components," *Progress in Additive Manufacturing*, Vol. 4, 2019, pp. 83–95. https://doi.org/10.1007/s40964-018-0061-3.

[14] Leishman, J. G., *Principles of Helicopter Aerodynamics*, 2nd ed., Cambridge University Press, 2006.

[15] Mandoc, K., et al., "Study on Noise Reduction for Drone Polymeric Propellers," *Macromolecular Symposia*, Vol. 404, No. 1, 2022, Article 2100483.

[16] 3DXTech, "CarbonX Nylon 6+CF Technical Data Sheet: High-Performance Carbon Fiber Reinforced PA6 for Structural Applications," 3DXTech, 2024, https://www.3dxtech.com/products/carbonx-nylon-6-cf-1.

[17] Fastl, H., and Zwicker, E., *Psychoacoustics: Facts and Models*, 3rd ed., Springer, 2007.